Engineering Turbulence Modelling and Experiments 3
W. Rodi and G. Bergeles (Editors)
© 1996 Elsevier Science B.V. All rights reserved.

Low-Reynolds-Number Eddy-Viscosity Modelling Based on Non-Linear Stress-Strain/Vorticity Relations

F.S. Lien, W.L. Chen and M.A. Leschziner
Department of Mechanical Engineering UMIST, Manchester, M60 1QD, UK

Abstract
High-Re forms of eddy-viscosity models based on non-linear relationships between the Reynolds stresses and the strain as well as vorticity tensors are extended to low-Re conditions along a novel route ensuring an asymptotic near-wall variation of turbulence length scale that is consistent with a particular one-equation model. The predictive performance of linear, quadratic and cubic forms is then investigated by reference to four flows featuring, inter alia, curvature, transition, impingement and separation. In particular, the role of the quadratic and cubic fragments is examined to determine their separate contribution to predictive realism.

1. INTRODUCTION

Eddy-viscosity models based on the linear Boussinesq relations are known to be afflicted by numerous weaknesses, including an inability to capture anisotropy, insufficient sensitivity to secondary strains, seriously excessive generation of turbulence at impingement zones and a violation of the realisability constraints at large strain rates. Notwithstanding the above defects, eddy-viscosity models remain popular, and their use in complex flows is widespread due, principally, to their formalistic simplicity, numerical robustness, and computational economy. Second-moment closure, on the other hand, accounts for several of the key features of turbulence which are misrepresented by linear eddy-viscosity models, but is considerably more complex and can suffer from low numerical stability due to the lack of dominance of second-order fragments in the set of terms representing diffusion. As a result, the CPU requirements for such closure models can be high, especially in 3D flows.

A potential alternative to second-moment closure, but one which retains important elements of the linear eddy-viscosity framework, is one which is based on constitutive relations linking the Reynolds-stresses to non-linear expansions of strains and vorticity components. These may be cast in a form of additive terms, each pre-multiplied by an apparent viscosity - hence the term 'non-linear eddy-viscosity models'. Examples include the models of Speziale [1], Shih et al [2] and Suga et al [3]. The stress-strain relationship for the first two variants, both high-Re forms, are truncated at the quadratic level. The third is more elaborate, includes the complete cubic term, is applicable to low-Re regions and is sensitising C_μ to S, Ω and A_2. The last term - the second stress invariant - is obtained by solving a related transport equation with fragments consistent with second-

moment closure.

The present paper uses high-Re non-linear eddy-viscosity models as a basis for formulating low-Re variants thereof, in which the effects of viscosity are treated via the length-scale formulation of Norris & Reynolds [4]. The modelling route taken essentially follows that proposed by Lien & Leschziner [5,6] in the context of the linear eddy-viscosity framework. In addition, the new forms adopt ideas proposed by Shih et al and Suga et al in respect of sensitising the eddy-viscosity directly to strain and vorticity invariants, and the effects arising from the cubic terms for a variety of flow conditions are examined thoroughly. The resulting unified approach is simple, easy to implement and performs well in both transitional and fully turbulent flows.

2. TURBULENCE MODELS

Based on series-expansion arguments, a general and coordinate invariant relationship between stresses and strains can be written as [7]:

$$\frac{\overline{u_i'u_j'}}{k} = \frac{2}{3}\delta_{ij} - \frac{\nu_T}{k}S_{ij} + C_1\frac{\nu_T}{\epsilon}[S_{ik}S_{kj} - \frac{1}{3}\delta_{ij}S_{kl}S_{kl}]$$

$$+C_2\frac{\nu_T}{\epsilon}[\Omega_{ik}S_{kj} + \Omega_{jk}S_{ki}] + C_3\frac{\nu_T}{\epsilon}[\Omega_{ik}\Omega_{jk} - \frac{1}{3}\delta_{ij}\Omega_{kl}\Omega_{kl}] + HOT, \tag{1}$$

where C_μ and C_1 to C_3, proposed by Shih et al [2] and applicable only to high-Re region, are

$$C_\mu = \frac{0.667}{A_1 + S + 0.9\Omega}|_{A_1=1.25}, \tag{2}$$

$$C_1 = \frac{3/4}{(1000 + S^3)}, \quad C_2 = \frac{15/4}{(1000 + S^3)}, \quad C_3 = \frac{19/4}{(1000 + S^3)}, \tag{3}$$

and

$$S_{ij} = \frac{\partial u_i}{\partial x_j} + \frac{\partial u_j}{\partial x_i}, \quad \Omega_{ij} = \frac{\partial u_i}{\partial x_j} - \frac{\partial u_j}{\partial x_i}, \quad S = \frac{k}{\epsilon}\sqrt{\frac{1}{2}S_{ij}S_{ij}}, \quad \Omega = \frac{k}{\epsilon}\sqrt{\frac{1}{2}\Omega_{ij}\Omega_{ij}}. \tag{4}$$

To examine the effect of streamline curvature on turbulence, a third-order correction suggested by Suga (1993) is also included, giving rise to

$$HOT = C_4\frac{\nu_T k}{\epsilon^2}(S_{ki}\Omega_{lj} + S_{kj}\Omega_{li})S_{kl} + C_5\frac{\nu_T k}{\epsilon^2}(S_{kl}S_{kl} - \Omega_{kl}\Omega_{kl})S_{ij} \tag{5}$$

where $C_4 = -10C_\mu^2$ and $C_5 = -2C_\mu^2$.[1]

The turbulent viscosity ν_T, arising from $k-\epsilon$ modelling framework, is

$$\nu_T = C_\mu\frac{k^2}{\epsilon}. \tag{6}$$

[1]The original value for C_5 is $-5C_\mu^2$, which is found to be too strong for highly separated flow.

In order to account for the semi-viscous near-wall effect, a damping function f_μ is introduced into (6), which, by reference to Norris/Reynolds' one-equation model [4], can be derived as [6]:

$$f_\mu = [1 - \exp(-0.0198y^*)](1 + \frac{5.29}{y^*}), \tag{7}$$

where $y^* = y\sqrt{k}/\nu$.

The dissipation rate ϵ is obtained from the solution of a related transport equation:

$$C_\epsilon - D_\epsilon = \frac{\epsilon}{k}(C_{\epsilon 1}P_k - C_{\epsilon 2}\epsilon), \tag{8}$$

where

$$C_{\epsilon 1} = 1.44(1 + P'_k/P_k), \quad C_{\epsilon 2} = 1.92[1 - 0.3\exp(-R_T^2)] \tag{9}$$

and $R_T = k^2/\nu\epsilon$. The P'_k is introduced to ensure that the correct level of near-wall turbulence-energy dissipation is returned. Then, by neglecting the C_ϵ, D_ϵ and P_k within the viscous sublayer,

$$P'_k = \frac{C_{\epsilon 2}\epsilon}{C_{\epsilon 1}}. \tag{10}$$

To improve the model's performance for transitional flow, the model has been modified to return, very close to the wall,

$$\epsilon = \underline{P_k} + 2\nu\frac{k}{y^2}, \tag{11}$$

where the underlined term P_k is used to replace the original proposal, $k^{3/2}/2.45y$, which is identical to the former but only in the local equilibrium condition. Finally, a damping function in the form of $\exp(-Cy^{*2})$ is introduced to ensure P'_k vanishes as $y^* \sim O(10^2)$, with the coefficient C correlated with log-law of the wall in fully-developed channel flow. The result is:

$$P'_k = 1.33[1 - 0.3\exp(-R_T^2)][P_k + 2\nu\frac{k}{y^2}]\exp(-0.00375y^{*2}) \tag{12}$$

It is appropriate to acknowledge that the use of the wall-normal distance in the present form of the ϵ-equation is an undesirable feature, with a view to its application to complex geometries. On the other hand, the equation does not include, in contrast to distance-free forms (e.g. [8]), terms of the type $2\nu(\frac{\partial^2 u}{\partial x_k \partial x_l})^2$ which are difficult to expand in general 3D coordinates and also provoke a high level of sensitivity to near-wall grid resolution.

3. NUMERICAL APPROACH

The above modelling practices have been implemented into a general non-orthogonal, collocated, block-structured finite-volume code (STREAM) in which convection of

momentum and turbulence quantities is approximated, respectively, with the quadratic upwind-biased scheme QUICK and a TVD formulation there of (the "UMIST" scheme). The nature and performance of this algorithm, used in conjunction with eddy-viscosity models as well as second-moment closure, both for incompressible and compressible (transonic) conditions, are documented in detail in [9-11].

4. RESULTS

The predictive performance of the modelling proposals summarised in Section 2 is investigated here by reference to four flows: a curved-channel flow, a transitional boundary layer, a cascade-blade flow and a separated flow behind a 2D hill.

The first case is a fully-developed curved-channel flow, at $Re = 70,000$ examined experimentally by Ellis & Joubert [12].

With turbulence effects represented by cubic stress-strain relations, the shear stress in a fully-developed curved shear flow, expressed in cylindrical coordinates, can be shown to be given by [13]:

$$\overline{u'_\theta u'_r} = -\nu_T[1 - C_5(S^2 - \Omega^2)](\frac{\partial u_\theta}{\partial r} - \frac{u_\theta}{r}). \tag{13}$$

It can be easily shown that for the present flow $S^2 - \Omega^2 = -4\frac{k^2}{\epsilon^2}\frac{\partial u_\theta}{\partial r}\frac{u_\theta}{r}$, and the distribution of S and Ω given in Fig. 1(a) shows that $S^2 - \Omega^2$ changes sign across the channel. This demonstrates that the cubic fragment, rather than the quadratic one, is important for capturing the interaction between streamline curvature and turbulence. Thus, curvature-related attenuation in shear stress, and hence turbulence production, arises over a convex surface, while amplification takes place on a concave wall. However, the mechanism by which the cubic fragment mimics curvature/turbulence interaction is very different from the real one which emerges from the exact transport equations for the Reynolds stresses. In the latter, the interaction is due, principally, to the retention of the exact production terms. For example, close to convex surface $P_{r\theta} = (\overline{u'^2_\theta} - \overline{u'^2_r})\frac{u_\theta}{r}$ and $P_{\theta\theta} - P_{rr} = -4\overline{u'_\theta u'_r}\frac{u_\theta}{r}$. Hence, an increase in the shear stress $\overline{u'_\theta u'_r}$ decreases the difference in $P_{\theta\theta} - P_{rr}$. This, in turn, reduces the level of shear-stress production - a negative feedback, leading to continuous attenuation of turbulence energy. Also, relation (13) is valid only if effects arising from normal-stress gradients are negligible, which is not the case, in general.

Fig. 1(b) compares velocity profiles predicted on a grid of 5,700 nodes with the linear Launder-Sharma model, the cubic model of Suga and the present cubic variant extended to low-Re conditions as proposed in Section 2. As seen, the present formulation returns a result which is close to that predicted by Suga's model. Although both clearly capture the asymmetry associated with turbulence attenuation and amplification, neither model gives the correct behaviour close to the inner, convex wall at which the boundary layer is clearly too thick. As is shown in Fig. 1(c), the cubic model returns a strong attenuation of turbulence energy at the inner wall and a moderate amplification at the outer one. Coupled with the result in Fig. 1(b), this suggests that the cubic fragment does not provide a quantitatively correct sensitivity to curvature, yielding excessive stabilisation along convex surfaces.

The second case is a transitional flow over a flat plate with variable pressure gradient imposed by profiling the opposite tunnel wall. This is known as the "T3C" test case, one of several being considered within a collaborative validation exercise coordinated by the ERCOFTAC Special Interest Group on Transition [14]. The free-stream velocity is $U_\infty = 6.2$ m/s, its turbulence intensity is $Tu = 8\%$, and the dissipation length scale is given by L_ϵ^∞=7 mm, the last so chosen as to achieve the correct rate of turbulence decay in the free stream. Results for skin friction, shape factor, streamwise velocity and turbulence-intensity profiles have been obtained with 31,000 nodes and are shown in Fig. 2. All models investigated are seen to give comparable performance, with the present linear as well as non-linear variants giving a slightly better representation than Launder & Sharma's linear model, the last often said to be the best eddy-viscosity model for resolving bypass transition [14]. Since no curvature is present in this flow, the contribution of the non-linear fragments is insignificant, and variations in the results are mainly due to minor differences in the value of C_μ.

The third case considered here is a turbulent flow over a double circular arc (DCA) compressor cascades measured by Zierke & Deutsch [15]. Computations have been performed with 48,000 nodes for an inlet-flow incidence angle of 5°, representing a particularly challenging off-design condition in which the flow is stalled on the blade's suction side. In this particular case, consideration will be given, separately, to the response of sensitising C_μ to strain and vorticity, of adopting different A_1 values in Eq. (1), and of using quadratic rather cubic constitutive stress-strain relations.

Velocity profiles on the suction side, predicted with a linear form of the model in Section 2 and $C_\mu = 0.09$ or the modified form $C_\mu = \frac{0.667}{A_1+S+0.9\Omega}|_{A_1=1.25}$ are compared in Fig. 3(a) with experimental data. Due to large normal strain rates generated in the vicinity of impingement point, close to the leading edge, the linear model with $C_\mu = 0.09$ produces excessive level of turbulence energy in this region through the production rate P_k $(= C_\mu \epsilon S^2)$. The $S - \Omega$-sensitised form of C_μ reduces this production substantially. As a consequence, the laminar separation bubble close to the leading edge is resolved, although experiment suggests that the separation bubble is very short. This initial test illustrates, principally, the inadequacy of using a constant C_μ in conjunction with the linear stress-strain relationship. One route to alleviating this defect is to express C_μ as a function of S and Ω in order to suppress the shear stress at the stagnation point and hence the turbulence energy.

Since boundary-layer separation is very sensitive to the level of shear stress, especially in the outer region of the boundary layer, a change in the value of A_1 in Eq. (1) can have a profound effect on the ability of a model using this form of C_μ to predict stall over a curved suction surface, as demonstrated by Lien & Leschziner [16]. However, this is an *ad-hoc* change which, while motivated by the need to sensitise the stresses to curvature strain, is in no way fundamentally related to flow curvature. It is precisely this observation which has motivated the formulation of non-linear models. It is interesting, therefore, to contrast the effect arising from modifying C_μ with that rendered by the cubic terms in the non-linear framework, which are responsible for curvature-related sensitivity. This is done in Fig. 3(a) by reference to contours $C_5(S^2 - \Omega^2)$ given in Fig. 3(b). It is seen that $A_1 = 1.25$, when used in conjunction with the cubic terms, predicts the correct streamwise

velocity profile at $x/c = 2.6\%$, which suggests the flow reattachment ahead of this location is correctly predicted. This is due to $S^2 - \Omega^2 > 0$ near the stagnation region, in which case the cubic term counteracts the effect arising from the functional dependence of C_μ on S and Ω. However, close to the trailing edge - say, at $x/c = 94\%$, the cubic variant returns a behaviour that is close to that arising from the quadratic form in which $A_1 = 4$, and this is due to largely negative values of $C_5(S^2 - \Omega^2)$ contours in the boundary layer on the suction side. That is, an elevation of A_1 from 1.25 to 4 is broadly equivalent to the effect introduced by the cubic fragment, although there is no physical connection between the two.

The last configuration is a turbulent flow over a 2D hill measured by Almeida et al [17], with massive separation present in the rear part of the hill. Computations were performed on a grid of 13,500 nodes, with very careful attention paid to resolution and to matching the upstream boundary conditions to the experimental data.

Contours of stream-function and of $C_5(S^2 - \Omega^2)$ and profiles of mean-velocity and turbulence quantities are given in Fig. 4. Fig. 4(a) demonstrates that the linear model under-predicts the size of the separation bubble, while the quadratic variant over-estimates it. The cubic variant returns almost the correct bubble size, which is somewhat surprising in view of the fact that the cubic fragment is expected to increase sensitivity to streamline curvature. Reference to the contours of $C_5(S^2 - \Omega^2)$ in Fig. 4(b) suggests that the curved shear layer emanating from the crest of the hill passes mainly through a region where $S^2 - \Omega^2$ is negative. However, $S^2 - \Omega^2$ is positive close to the separation point, which might be due to a strong deceleration in that region, caused by too much entrainment from the free stream and resulting in early flow reattachment. Consistent with the above observation are the profiles of streamwise velocity and shear-stress given in Fig. 4(c). Thus, the cubic variant returns slightly higher levels of shear stress across the curved shear layer compared to the quadratic one. As a result of the correct reattachment point, the cubic model also performs better in the recovery region. It is further observed that the non-linear models yield higher $\overline{u'^2}$ than the linear variant, which is indicative of the inherent ability of the former group to capture anisotropy through the inclusion of the *traceless* non-linear fragments. This applies to both quadratic and cubic forms, although in the former, the linkage between anisotropy and shear stress is unrealistically weak (in fact, non-existent in homogeneous shear).

5. CONCLUSIONS

Computational studies have been undertaken for a wide range of flow conditions to investigate the predictive capabilities of new forms of non-linear eddy-viscosity models which have emerged as extensions of the high-Re variant of Shih et al to low-Re conditions using concepts previously applied by the authors to the linear k-ϵ framework. It has been demonstrated that the inclusion of non-linear fragments allows turbulence anisotropy to be predicted. However, the interaction between shear and wall-normal Reynolds stresses is weak, especially if only quadratic fragments are included. At impingement and separated zones, the desirable reduction of shear stress, relative to that returned by the linear form, is mainly due to the functional dependence of $C_\mu(S, \Omega)$. The cubic fragments enhance, contrary to the desired response, the turbulence level in stagnation regions, but mimics,

qualitatively, the sensitivity to streamline curvature in relatively simple flows. The level of this sensitivity is not entirely correct, however, and the model does not represent the associated physical mechanism in a fundamentally correct manner. In more general flows in which strain fields are complex and in which contributions from normal strains are substantial, the way in which non-linear models represent the interaction between turbulence and streamline curvature may not be adequate across the whole flow domain.

REFERENCES

[1] Speziale, C.G. (1987), *J. Fluid Mech.*, Vol. 178, p. 459.

[2] Shih, T.H., Zhu, J. and Lumley, J.L. (1993), "A Realisable Reynolds Stress Algebraic Equation Model", *NASA TM-105993.*

[3] Suga, K., Craft, T.J. and Launder, B.E. (1994), "Development and Application of a Non-Linear $k - \epsilon$ Model", *Proc. 6th Biennial Colloquium on CFD*, UMIST.

[4] Norris, L.H. and Reynolds, W.C. (1975), "Turbulence Channel Flow With a Moving Wavy Boundary", *Rep. FM-10*, Dept. of Mech. Engrg., Stanford University.

[5] Lien, F.S. and Leschziner, M.A. (1993), *Engineering Turbulence Modelling and Measurements 2*, Elsevier, p. 217.

[6] Lien, F.S. and Leschziner, M.A. (1995a), *ASME Paper 95-CTP-80.*

[7] Pope, S.B. (1975), *J. Fluid Mech.*, Vol. 72, p. 331.

[8] Launder, B.E. and Sharma, B.I. (1974), *Letters in Heat and Mass Transfer*, Vol. 1, p. 131.

[9] Lien, F.S. and Leschziner, M.A. (1994), *Comp. Meth. Appl. Mech. Eng.*, Vol. 114, p. 123 and p. 149.

[10] Lien, F.S. and Leschziner, M.A. (1994), *Int. J. Num. Meth. Fluids*, Vol. 19, p. 527.

[11] Lien, F.S., Chen, W.L. and Leschziner, M.A. (1995), "A Multi-Block Implementation of a Non-Orthogonal, Collocated Finite-Volume Algorithm for Complex Turbulent Flows", *Report TFD/95/06*, Dept. of Mech. Eng., UMIST.

[12] Ellis, L.B. and Joubert, P.N. (1974), *J. Fluid Mech.*, Vol. 62, p. 65.

[13] Suga, K. (1993), "Eddy Viscosity Modelling With Deformation Invariants and Non-Linear Elements", *First-Year Ph.D Report*, Dept. of Mech. Eng., UMIST.

[14] Savill, A.M. (1993), *Engineering Turbulence Modelling and Measurements 2*, Elsevier, p. 583.

[15] Zierke, W.C. and Deutsch, S. (1989), "The Measurement of Boundary Layers on a Compressor Blade in Cascade", *NASA CR 185118.*

[16] Lien, F.S. and Leschziner, M.A. (1995), *Aeronautical J.*, Vol. 99, p. 125.

[17] Almeida, G.P., Durao, D.F.G. and Heitor, M.V. (1993), *Exp. Thermal and Fluid Science*, Vol. 7, p. 87.

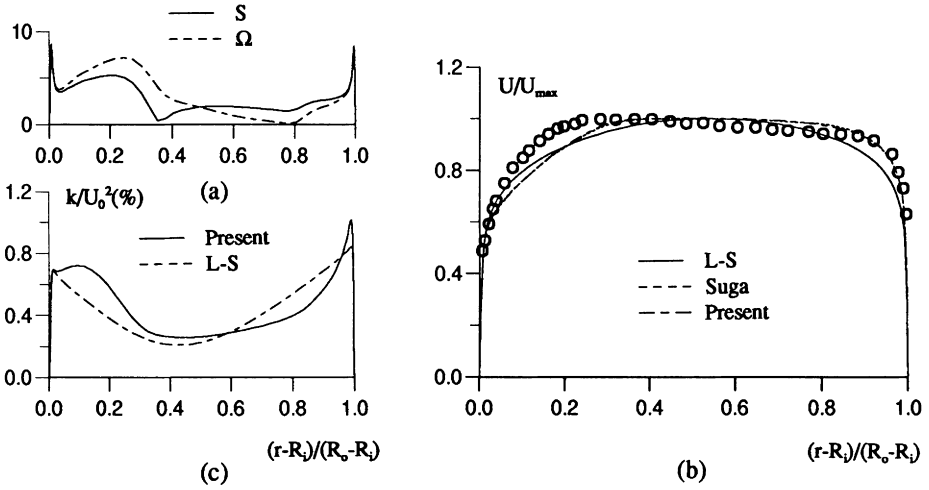

Figure 1: Fully-developed flow in curved channel: (a) variation of strain and vorticity invariants; (b) velocity profiles; (c) turbulence-energy profiles

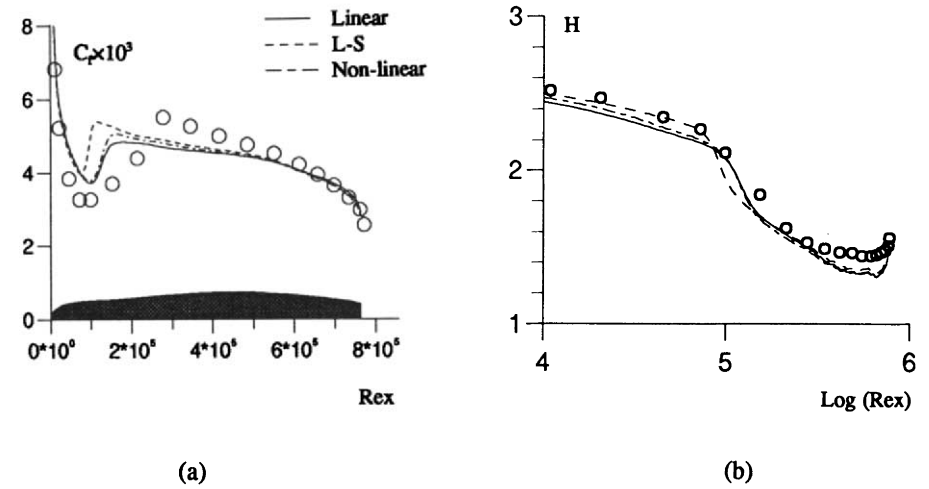

Figure 2: Transitional flat-plate boundary layer: (a) skin-friction variation; (b) shape-factor variation

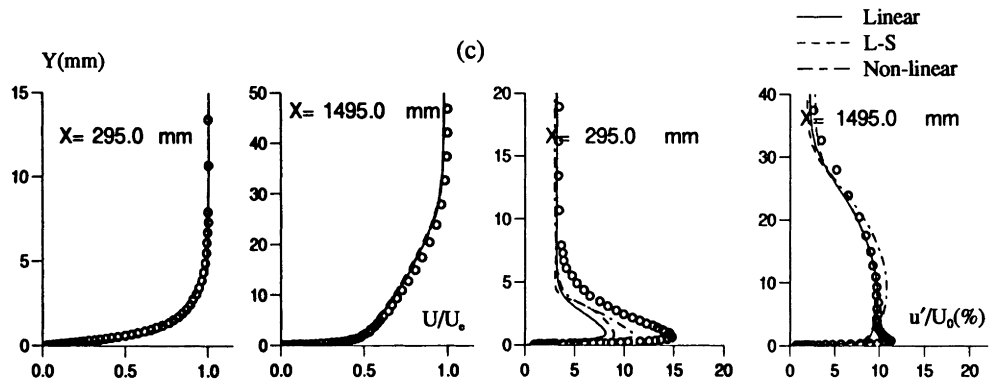

Figure 2: Transitional flat-plate boundary layer (cont): (c) streamwise velocity and turbulence-intensity profiles

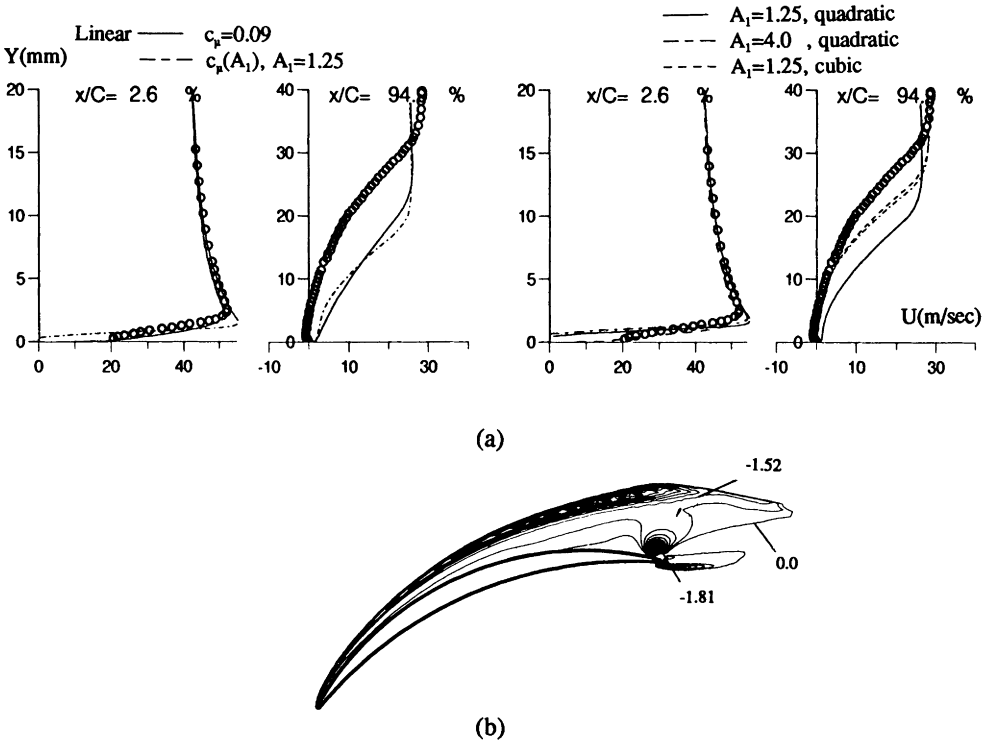

Figure 3: Flow over a compressor-cascade blade: (a) velocity profiles on the suction side; (b) negative values of $C_5(S^2 - \Omega^2)$-contours

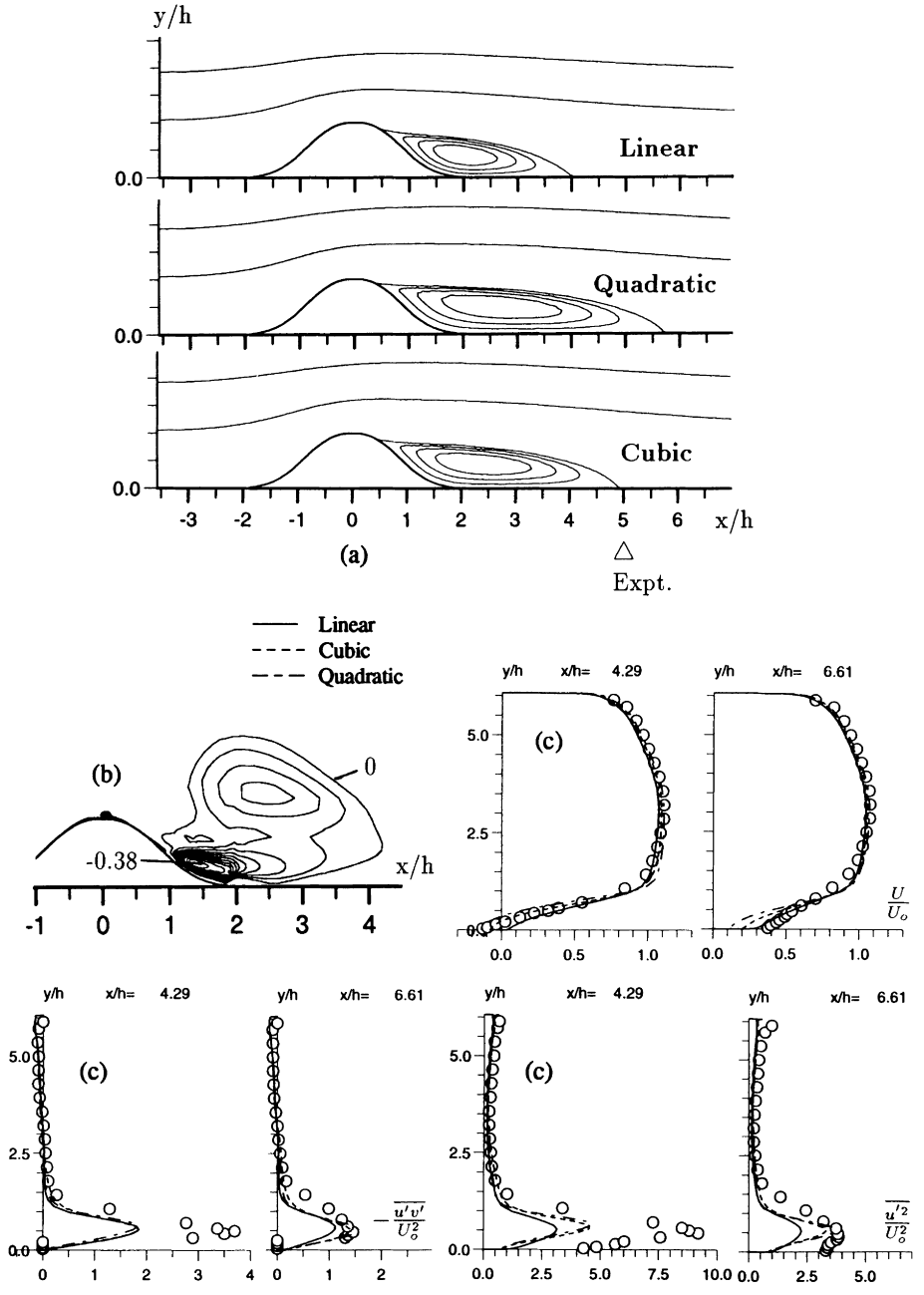

Figure 4: Flow over a hill: (a) streamfunction contours; (b) negative values of $C_5(S^2 - \Omega^2)$-contours; (c) profiles of velocity and Reynolds-stresses